

## Beta Particle Energy Spectra Shift due to Self-attenuation Effects in Environmental Sources

Thomas Alton<sup>1</sup>, Dr Stephen David Monk<sup>1</sup>, Dr David Cheneler<sup>1</sup>

<sup>1</sup> Engineering Department, Lancaster University, Lancaster, United Kingdom, LA1 4YW

Corresponding author details:

Name: Dr David Cheneler

e-mail: [d.cheneler@lancaster.ac.uk](mailto:d.cheneler@lancaster.ac.uk)

### Abstract

In order to predict and control the environmental and health impacts of ionising radiation in environmental sources such as groundwater, it is necessary to identify the radionuclides present. Beta-emitting radionuclides are frequently identified by measuring their characteristic energy spectra. The present work shows that self-attenuation effects from volume sources result in a geometry-dependent shift in the characteristic spectra which needs to be taken into account in order to correctly identify the radionuclides present. These effects are shown to be compounded due to the subsequent shift in the photon spectra produced by the detector, in this case an inorganic solid scintillator ( $\text{CaF}_2:\text{Eu}$ ) monitored using a Silicon Photomultiplier (SiPM). Using tritiated water as an environmentally relevant, and notoriously difficult to monitor case study, analytical predictions for the shift in the energy spectra as a function of depth of source have been derived. These predictions have been validated using Geant4 simulations and experimental results measured using bespoke instrumentation.

**Key Words:** Scintillator, Tritium, Geant4, Attenuation

### Introduction

When present in environmental sources such as groundwater, beta particle emitting radioisotopes can have significant negative health implications. As such, pertinent industries, such as the nuclear industry, need to ensure that the concentration of these radionuclides is kept below safe levels. For instance, the current World Health Organisation (WHO) concentration limit for tritium in groundwater is 10,000 Bq/L [1], while the European Union has an investigative level of 100 Bq/L [2]. However, detection of low-energy beta particles in water is difficult owing to the short distances these particles travel before being absorbed. This particularly true of tritium which decays with a very low energy beta (<18.6 keV), but nonetheless can still have negative health implications. While this manuscript focuses on tritium due to the importance and difficulty in measuring tritium, all conclusions apply quite generally to other low-energy beta particle emitting radioisotopes.

Besides the low energy of the emitted beta particles, tritium is also difficult to detect because of its chemistry. Tritium is an isotope of hydrogen commonly found in the form of tritiated water. This is where the  $^1\text{H}$  in  $^1_2\text{HO}$  can be replaced with  $^3\text{H}$  leading to either  $^3_2\text{HO}$  or  $^3\text{HO}^1\text{H}$  [3]. Therefore, in order to detect tritium directly, a method that can chemically differentiate between tritiated water and pure water is required. This is non-trivial and as such it is more usual to detect tritium by monitoring the energy spectrum of the emitted beta particles. The most frequently used method for accurate

determination of tritium in water is liquid scintillation counting. Use of liquid scintillation is inconvenient for in-situ, transient monitoring as samples need to be collected and mixed with the liquid scintillation cocktail and tested often in dedicated lab-based equipment. This is time consuming and expensive and has issues with chemical disposal as the cocktails are often toxic to aquatic life [4].

An alternative to using a liquid scintillation counter for detecting tritium in water is to use a solid scintillator. Solid scintillators are more convenient for in-situ monitoring of beta radiation as there is no need to mix samples with a scintillating cocktail. This means that solid scintillator based systems can be used to transiently monitor water sources and detect possible sources of contamination almost in real-time. A frequently used scintillator that is sensitive to low-energy beta particles is  $\text{CaF}_2:\text{Eu}$  [5]. A number of researchers (Kawano [6] [7], Shirahashi [8], Kozlov [9], Shul'gin [10] and Rudin [11]) have used  $\text{CaF}_2:\text{Eu}$  for the detection of tritium in water.  $\text{CaF}_2:\text{Eu}$  is particularly well suited to this purpose as it is non-hygroscopic, has a refractive index comparable to water and a light output comparable to  $\text{NaI:Tl}$  (30,000 photons per MeV compared to 37,000 photons per MeV produced using  $\text{NaI:Tl}$  [12]) which can't be used in contact with water as it is hygroscopic.

The primary advantage of liquid scintillation over solid scintillation techniques is that with the former, the distance the beta particle has to travel within the cocktail before interacting with a scintillating molecule is minimised. This reduces the effects of attenuation thus maximising efficiency. With solid scintillators, the beta particle must first travel through the volume of water before interacting with the scintillator, hence attenuation effects are profound. A number of studies have looked into the effects self-attenuation have on volume sources of gamma particles with a view of correcting the measured activity during gamma spectroscopy [13] [14]. These studies do not consider the change in the expected energy spectrum measured during spectroscopic experiments as a result of self-attenuation. Given that comparing the measured energy spectrum to the characteristic energy for a given radionuclide is a common way of identifying that radionuclide, this shift in the energy spectrum is of significant importance when monitoring unknown contamination in water sources. To this end, a theory that extends the current models of self-attenuation to the interaction of a large, potentially infinite, volume source of beta particles has been developed within this study. The current model also goes further than previous models by providing an explicit expression for the attenuated energy spectrum that will actually be measured.

This model has been validated for tritium within this study using Monte Carlo simulations that include the attenuation effects within beta particle transport. This was achieved using Geant4 version 10.1 [15]. Further validation was conducted using a bespoke solid scintillator detector incorporating  $\text{CaF}_2:\text{Eu}$  in contact with an SiPM. The output of the SiPM was correlated to the light produced by the scintillator by using a simplified form of the output pulse. Due to practical issues related to the low energy of the beta particles emitted by tritium, the experiments were further validated using simulations using another radioisotope, Chlorine 36, as it is a near pure beta emitter and produces higher energy beta particles (709 keV [16]). It is hoped that these models can be used to facilitate detector system designs capable of detecting low-energy beta particle emitting radioisotopes at low concentrations that would be found in environmental situations.

### **Theoretical Explanation of Beta Attenuation from a Volume Source**

Consider a cylinder scintillator in contact with the surface of a volume of tritiated water with activity density  $A$ . The scintillator has a radius  $R$  and length  $h$ . An elemental volume of the tritiated water, where  $dV = dx dy dz$  see Fig.1a, emits beta particles in all directions with equal probability. The attenuation and scattering of the beta particles as it travels through the water is captured to first order by a linear attenuation coefficient (in  $\text{cm}^{-1}$ ), denoted by  $\mu$ . Use of this coefficient assumes an

exponential decrease in kinetic energy as the particle travels through the medium [17]. The rate of flux,  $\Phi$ , of beta particles passing through area  $dS$  on the scintillator surface is the product of the number of beta particles emanating from volume  $dV$  per second per steradian and the solid angle subtended by the area element and the exponential attenuation factor:

$$d\Phi = \left(\frac{AdV}{4\pi}\right) \left(\frac{\hat{\mathbf{n}} \cdot dS}{d^2}\right) (e^{-\mu d}) = \frac{Ae^{-\mu d}}{4\pi d^2} \hat{\mathbf{n}} \cdot dS dV \quad \text{Eq. 1}$$

$d$  is the shortest distance from  $dV$  to  $dS$  and  $\hat{\mathbf{n}}$  is the unit vector from  $dS$  to  $dV$ . Setting the base of the scintillator to be perpendicular to the z-axis as shown in Fig.1, an elemental area on the base, positioned at  $(x,y,0)$ , can be denoted as  $dS = (0,0,1)dx dy$ . The rate of flux of beta particles emanating from volume  $dV$  and reaching area  $dS$  is therefore:

$$d\Phi = \frac{Ae^{-\mu d}}{4\pi d^2} \hat{\mathbf{n}} \cdot dS dV = \frac{Az_1 \exp\left(-\mu[(x-x_1)^2 + (y-y_1)^2 + z_1^2]^{1/2}\right)}{4\pi[(x-x_1)^2 + (y-y_1)^2 + z_1^2]^{3/2}} dx dy dz \quad \text{Eq. 2}$$

Therefore the total flux of beta particles that can reach the base of the scintillator is:

$$\Phi_D = \int_{-\infty}^0 \int_{-\infty}^{\infty} \int_{-\infty}^{\infty} \int_{-R}^R \int_{-\sqrt{R^2-x^2}}^{\sqrt{R^2-x^2}} \frac{Az_1 \left(-\mu[(x-x_1)^2 + (y-y_1)^2 + z_1^2]^{1/2}\right)}{4\pi[(x-x_1)^2 + (y-y_1)^2 + z_1^2]^{3/2}} dx dy dz \quad \text{Eq. 3}$$

In practice, as the energy of the beta particles is small, numerical integration of Eq.2 can be over a much smaller domain (i.e. non-infinite) than suggested and still get accurate results. To simply this integral, the axisymmetry of the problem can be exploited by setting  $x = r \cos\phi$ ,  $y = r \sin\phi$ ,  $dx dy = r dr d\phi$ ,  $x_1 = r_1 \cos\phi_1$ ,  $y_1 = r_1 \sin\phi_1$ ,  $dx_1 dy_1 = r_1 dr_1 d\phi_1$  yielding:

$$\Phi_D = \int_0^{2\pi} \int_0^{R_v} \int_0^R \int_{-H_v}^0 \frac{A r r_1 z_1 \left(-\mu[r^2 + r_1^2 - 2r r_1 \cos(\theta) + z_1^2]^{1/2}\right)}{4\pi[r^2 + r_1^2 - 2r r_1 \cos(\theta) + z_1^2]^{3/2}} dz_1 dr dr_1 d\theta \quad \text{Eq. 4}$$

This integral becomes singular when  $r^2 + r_1^2 - \cos(\theta) + z_1^2 = 0$  making it difficult to solve using brute force Monte Carlo and quadrature integration methods. This is because when  $z_1 \rightarrow 0$  and  $\cos(\theta) \rightarrow 1$ , the integral becomes singular when  $r \rightarrow r_1$  which is an area inconveniently in the middle of the domain of integration preventing good convergence using the previously mentioned methods. However, the Vegas algorithm [18] which utilises both importance sampling and adaptive stratified sampling as implemented in Python using the Vegas 3.0 algorithm [19] yields satisfactory results.

The mass attenuation was determined using the built in cross section files, the mean free path and therefore the mass attenuation can be determined. The mass attenuation is a function of the initial kinetic energy of the beta particle. The mass attenuation can be calculated from Geant4 using the mean free path data at various energies, when fitting to this data a standard power-law relationship is observed:

$$\left(\frac{\mu}{\rho}\right) = \frac{1.28}{T^{1.74}} \quad \text{Eq. 5}$$

where  $T$  is the initial kinetic energy of the beta particle in MeV and  $\rho$  is the density of water  $\text{g/cm}^3$ . The coefficient in Eq.6 are  $1.28 \pm 0.0390$  and  $1.74 \pm 0.0061$  respectively where the errors denote a 95% confidence level. The coefficient of determination [20] for the fit is 0.938 (See Fig.1b).

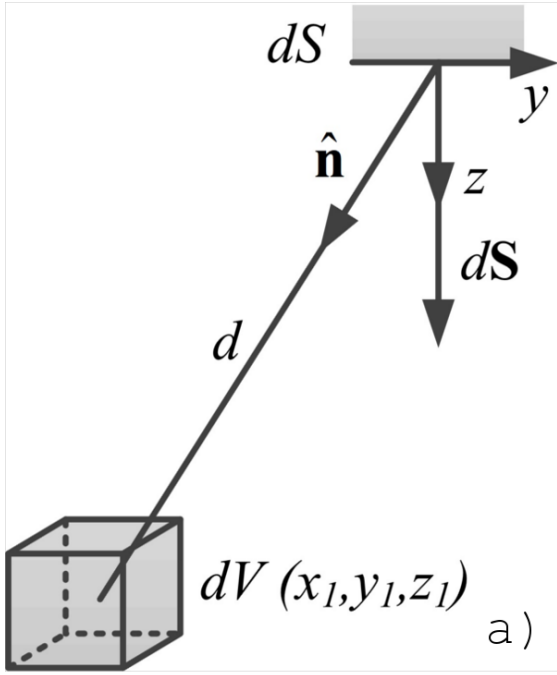
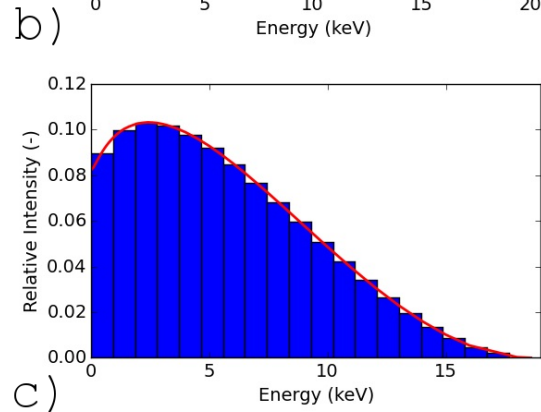
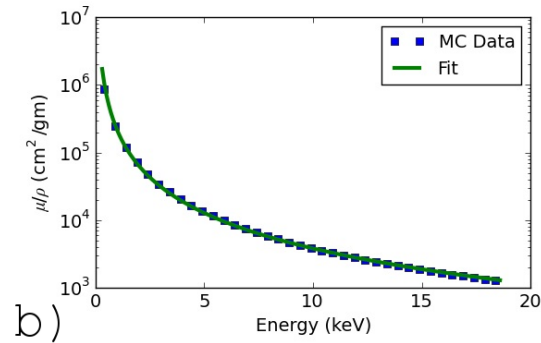


Fig.1: a) Geometry of beta particle interaction from a volume of tritiated water,  $dV$ , to an area on the scintillator  $dS$ .  $d$  is the shortest distance from  $dV$  to  $dS$  and  $\hat{n}$  is the unit vector from  $dS$  to  $dV$ . b) Comparison of the mass-attenuation of beta particles in water as calculated by Eq.6 (solid line) and that provided by Geant4 (squares). c) Probability mass function of the relative intensity of beta particles emitted with a given initial kinetic energy  $T_i$ . The red line denotes the continuous relative distribution  $N(T)$ . Note  $k=20$  for this figure, however it was 1000 during subsequent calculations.



The beta particles are emitted from the tritiated water with a spectrum of possible energies as shown in Fig.1c. This can be conveniently presented by a probability mass function so that the  $i^{th}$  group of beta particles can be treated as a monoenergetic beam with initial kinetic energy:

$$T_i = \frac{Q}{k} \left( i - \frac{1}{2} \right) \quad \text{Eq. 6}$$

where  $Q$  is the maximum kinetic energy (18.59keV) and  $k$  is the total number of groups. The relative emitted intensity, i.e. the proportion of beta particles that are emitted with kinetic energy  $T_i$  can be shown to be:

$$I_i = \frac{\int_{T_{i-1/2}}^{T_{i+1/2}} N(T) dT}{\int_0^Q N(T) dT} \quad \text{Eq. 7}$$

where  $N(T)$  is the energy spectrum for tritium. In this way, the energy spectrum can be represented in Fig.1c. The flux on the scintillator surface due to beta particles of initial kinetic energy  $T_i$  being emitted over the entire volume of tritiated water is therefore:

$$\Phi_i = \int_0^{2\pi} \int_0^{R_v} \int_0^R \int_{-H_v}^0 \frac{A I_i r r_1 z_1 \exp\left(-\mu[r^2 + r_1^2 - 2rr_1 \cos(\theta) + z_1^2]^{\frac{1}{2}}\right)}{2[r^2 + r_1^2 - 2rr_1 \cos(\theta) + z_1^2]^{\frac{1}{2}}} dz_1 dr dr_1 d\theta \quad \text{Eq. 8}$$

The total flux is defined simply as:

$$\Phi_T = \sum_{i=0}^k \Phi_i \quad \text{Eq. 9}$$

The attenuated energy spectrum of the beta particles colliding with the scintillator surface is:

$$N_A = \sum_{i=0}^k \left( T_i \Phi_i \frac{1}{n} \sum_{j=0}^n \exp(-\mu_i d_j) \right) \quad \text{Eq. 10}$$

for all  $d_j$ . This can be calculated by randomly generating a list of  $n$  (where  $n$  is very large, here  $10^6$  was used) pairs of coordinates, where one set of coordinates spans the whole volume of tritium and the other set is over the entire surface of the scintillator.

#### Geant4

Geant4 is Monte Carlo simulation software written by CERN to model nuclear and particle physics. Geant4 (version 10.1) supports physics for low energy beta particles (verified down to 1keV), optical photon tracking and the process of scintillation. Simulations of scintillation, beta particle and photon transport were conducted using the EM Standard [21], which includes effects of ionization, scintillation, bremsstrahlung, multiple scattering and Compton scattering. Initial energy spectra for  $^3\text{H}$  and  $^{36}\text{Cl}$  was taken from the Radiological Toolbox [22] and inputted into the simulations as a 1000 bin normalised histogram.

An initial simulation was conducted in order to ascertain the range of beta particles emitted by tritium in both water and the scintillator ( $\text{CaF}_2:\text{Eu}$ ) in order to guide future simulations and experimental designs. Geant4 calculates the length a particle travels as a series of steps; the range is then deduced as the sum of the straight line distance between interactions along with a correction for scattering. The simulation has a cut off in distance, but will track primary particles down to low energies ( $\sim 60$  eV). The lengths the primary particles travel in the material is then the penetration length or range. Each material was simulated separately as a 40 cm cube with a beta particle point source in the centre. As can be seen in Fig. 2a, the maximum ranges of the beta particles emitted by tritium are *c.a.* 7  $\mu\text{m}$  and 3  $\mu\text{m}$  in water and  $\text{CaF}_2:\text{Eu}$  respectively.

Of significant interest is the attenuated energy spectrum. This is the spectrum of beta particles interacting with the base of the scintillator. This cannot be measured directly as the beta particles must first be converted by scintillation to photons which are then detected. This spectrum is effectively the input to the detector system and incorporates all the effects of geometry and self-attenuation of the source. This spectrum can be calculated using Eq. 10. It was simulated using Geant4 using the geometry as shown in Fig. 2b. For this, the source was a cylindrical isotropic volume source of increasing thickness to better investigate the effects of attenuation. The tritium volume source was placed in contact with the scintillator to match the experimental setup. The attenuated beta particles resulted in a spectrum of photons produced in the scintillator. The number of photons interacting with the SiPM as a result of the initial tritium source was also recorded as this is the information that would ultimately be recorded experimentally. The results of this simulation are shown in the next section.

For validation the previous model was repeated using a  $^{36}\text{Cl}$  disc source with a 1 mm air gap between it and the scintillator. All water was removed so that there was no attenuation. This setup was chosen as it was experimentally convenient and could be used to validate the SiPM model.

#### Experimental Detector Setup

For further validation, a bespoke detector system with an approximate geometry shown in Fig. 2b was fabricated. This setup involved the use of a single crystal of  $\text{CaF}_2:\text{Eu}$  optically coupled to an SiPM; the output of the SiPM was connected to a charge sensitive preamplifier and then finally to an Analog to Digital Converter (ADC). A volume of tritiated water was placed in contact with the scintillator. Three concentrations of tritium (15, 150 and 1500 Bq/mL) were tested as was a test-case consisting of just

de-ionised water. This acted as a control and was used to measure the response of the system in the absence of ionising radiation. Additionally, a closed disc source of  $^{36}\text{Cl}$  (beta energy <709 keV) with an activity of 50 Bq was used as another test case. A disc source was placed 1 mm directly under the scintillator. In all cases, the electronics and source was placed inside of two light proof boxes to prevent exposure to external radiation.

Both the tritium and  $^{36}\text{Cl}$  experimental data was analysed by applying a peak finding code [23] to the output of the SiPM. This uses the derivative approach along with a threshold to determine the peak amplitude of recorded events as typified in Fig. 3a.

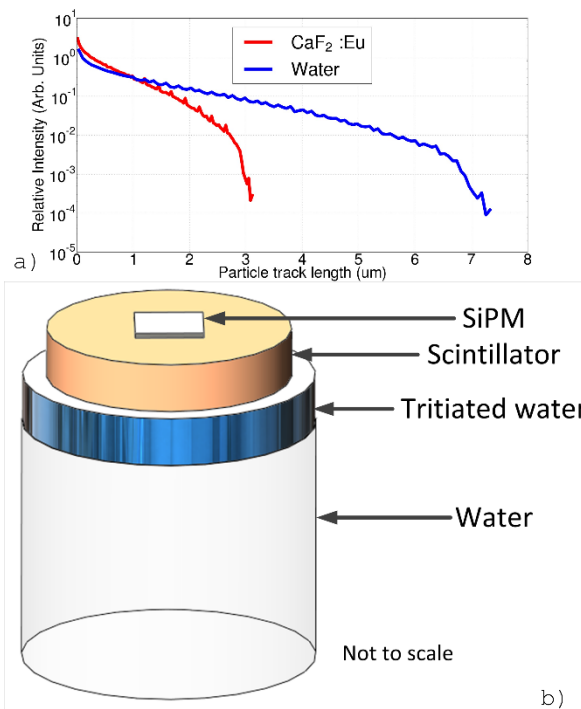


Fig.2: a) Figure showing the Penetration lengths for water and  $\text{CaF}_2:\text{Eu}$  for the tritium energy spectrum. b) Diagram of the detector for the Geant4 simulation 2.

The SiPM has been analysed previously ([24], [25]) and the equivalent circuit suggest a second order circuit. The simplest characteristic equation for such a system is given in eq. 11. In that equation,  $i(t)$  is the output current at a time  $t$ ,  $c$  is a scaling factor  $a$  and  $b$  are the rise and fall time constants.

$$i(t) = c(\exp(-t/a) + \exp(-t/b)) \quad \text{Eq. 11}$$

The equation describing the shape of the output pulse can be seen to be sufficiently accurate as it closely matches the data, as seen in Fig. 3a. Using the data from thirty events and curve fitting, the value  $a$  was determined to be  $2.381 \times 10^{-7} \pm 1.085 \times 10^{-9}$  s and the value of  $b$  was determined to be  $7.443 \times 10^{-7} \pm 2.283 \times 10^{-9}$  s with the errors being a 95% confidence level. It was shown that the time constants were indeed constant and independent of the amplitude of the energy of the event. For this data the coefficient of determination was 0.98.

The output voltage measured from the SiPM can be calculated from Eq. 11 to give:

$$V(t) = 1.8 \times 10^{19} \cdot G \cdot \frac{RQ \cdot CQ \cdot CD \cdot RS}{b - a} \cdot e \cdot (\exp(-t/a) - \exp(-t/b)) \quad \text{Eq. 12}$$

Where  $G$  is the gain,  $e$  is the charge on an electron,  $RQ$  is the quench resistance,  $CQ$  is the quench capacitance,  $CD$  is the capacitance in the circuit and  $RS$  is an assumed resistance. The values  $RQ$ ,  $CQ$  and  $CD$  are dependent on the number of arriving photons.

## Results and Discussion

### Geant4

The normalised attenuated beta particle energy spectrum for tritiated water that impinges on the scintillator as calculated by Geant4 is shown in Fig. 3b. As can be seen, the spectrum shifts from the original unattenuated spectrum as the source gets thicker and the attenuation effects increase. As shown in Fig. 2a, the maximum range of the beta particles emitted by tritium in water is *c.a.* 7.2  $\mu\text{m}$ . However, the spectrum is affected by increasing the depth of the source up to a depth of 5  $\mu\text{m}$ . This

is indicated in Fig. 3b by the convergence of the spectra of the 5  $\mu\text{m}$  and 10  $\mu\text{m}$  deep sources. These spectra are the same and do not change as the source gets deeper. Therefore, this is essentially the spectra one would expect to see when monitoring an effectively infinite tritiated water source. It should be noted that the actual maximum energy beta particle that can be detected has changed from the original 18.6 keV to *c.a.* 12 keV. Similarly, the average energy changed from 5.7 keV to *c.a.* 6.3 keV. It can be seen in Fig. 4a that the simulated data compares well to the theoretical prediction calculated using Eq. 10 assuming a semi-infinite source.

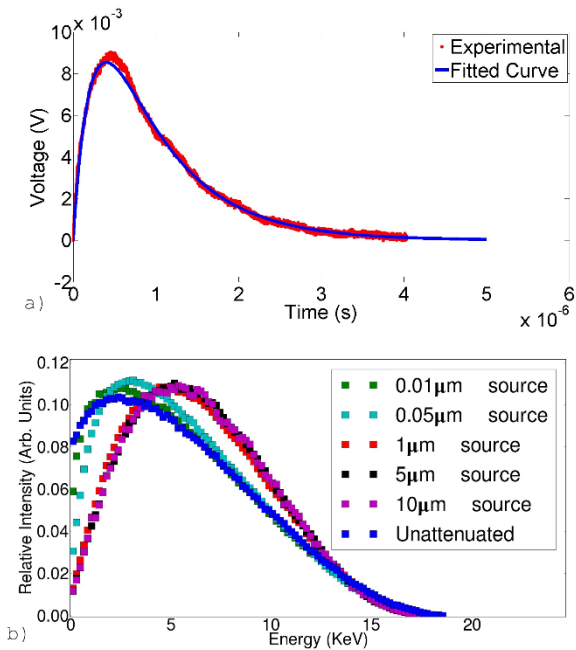


Fig.3: a) Typical raw data from the SiPM output due to a light pulse plotted against the fitted equation. b) Data showing the normalised energy spectrum of the beta particles entering the scintillator, the unattenuated data is the initial energy spectrum.

the simulations predict the shape of the measured spectra well. The results from both isotopes show a peak close to 0V which can be explained as the noise from the SiPM and electronics. The errors were calculated as  $1/\sqrt{N}$ , where N is the number of particles detected in each histogram bin. Errors in the experimental data are the result of background radiation, thermally generated electron/hole pairs in the SiPM, electronic noise and the data analysis code. For instance, both Fig4c & 4d show a peak at approx. -0.3V which then decreases in amplitude towards the 0V mark, this can be explained by the use of the threshold for the peak finding code, which was set to -0.265V during calibration.

## Conclusions

Knowledge of the energy spectrum of emitted beta particles is an important factor in the identification of radionuclides. It has been shown here, however, that the spectra emitted from environmental sources is not the same as that expected from a simple point source. The shift in the spectra due to self-attenuation has been predicted analytically allowing for more reliable identification of radionuclides. It was further shown that the shift in the spectra is dependent on the geometry of the source and depends on the relative distance a beta particle must travel before interacting with a scintillator within the source as compared to the maximum range of the particle. An important

The data in Fig. 4b shows how the attenuation affects the light production when comparing the quasi-infinite source to an unattenuated source. As can be seen in this figure the amount of light produced per event changes due to the self-attenuation of the beta particle along with a decrease in the maximum number of photons produced.

## Experimental Results

The photon output data generated using Geant4 simulations (e.g. Fig. 4b) can be compared directly with experiments by using this data to estimate  $N_{fired}$  and using Eq. 12 to estimate the output voltage of the SiPM. 80 minutes of data was collected from the SiPM under exposure of tritium and  $^{36}\text{Cl}$ . The peak finding algorithm as described above was used to ascertain the amplitude of the peaks corresponding to events (interaction between beta particles and the scintillator and the distribution of the peak amplitudes is presented as normalised histograms in Fig. 4c for tritium and Fig. 4d for  $^{36}\text{Cl}$ . These figures show that the

consequence of this shifted energy spectrum is that the distribution of photons produced within the scintillator is also changed. Therefore any scintillator based detector system developed will be need to be corrected for to include the effects of this shifted light distribution. Practical issues regarding the identification of events, i.e. the detected interaction of beta particles with a scintillator, were also discussed. In particular, a simplified form describing the output of the SiPM during such an event was given allowing for better identification of the event. The expression derived to calculate the attenuated spectrum of the beta particles emitted from a given radionuclide distributed in a self-attenuating volume source has been verified by comparing with Geant4 Monte Carlo simulations. These simulations were also used to predict the output of the detector system thus confirming the need to incorporate the effects of the spectrum shift.

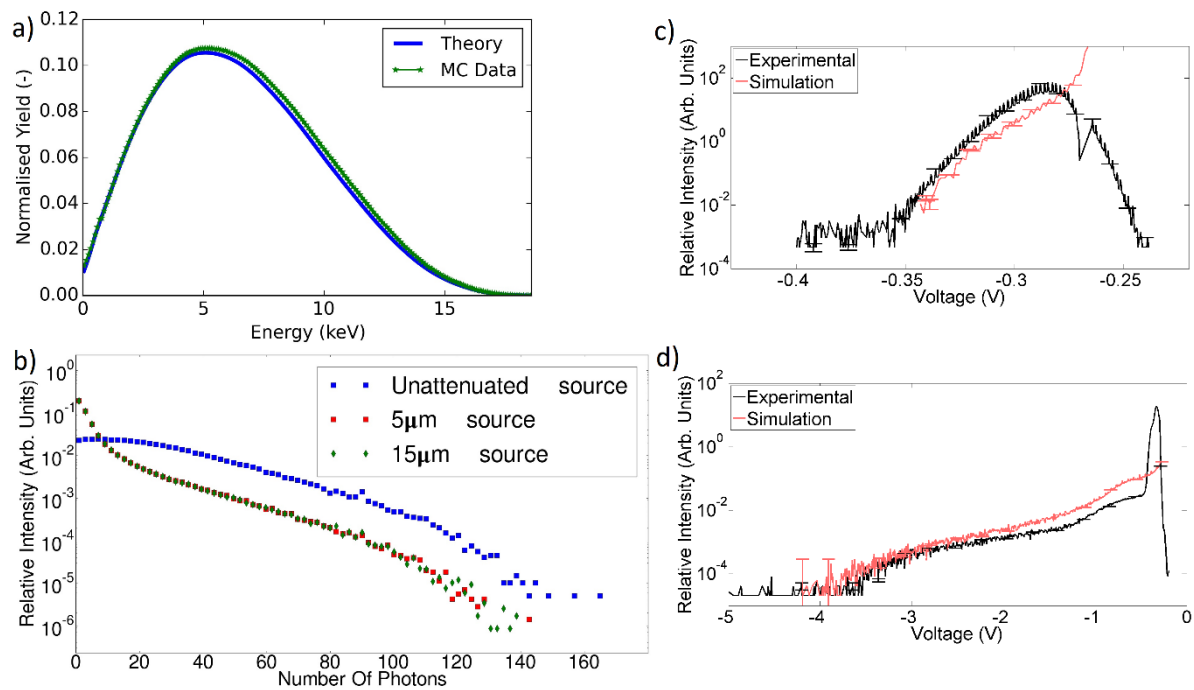


*Fig.4: a) Expected beta spectrum due to self-attenuation of beta particles by an infinite volume tritiated source on a solid scintillator. Solid blue line shows the spectrum calculated using Eq.10 for an infinite source and the green line with star markers denotes that calculated using Geant4 taken from the 15 μm deep source in Fig.3b. b) The number of photons produced per event that arrive into the SiPM. c) A comparison between the simulation data and experimental data for 80 minutes of the 1.5kBq/mL  $^3\text{H}$  source. Bin values of zero were omitted. d) A comparison between the simulation data and experimental data for 80 minutes of the  $\text{Cl}^{36}$  source. Bin values of zero were omitted.*

## Acknowledgements

The authors would like to thank the Lancaster University Faculty of Science and Technology for the funding for this research and also to thank Dr Jackie Pates of the Lancaster University LEC (Lancaster Environment Centre) for her advice.

## References

- [1] W.H. Organization, Guidelines for drinking-water quality, fourth edition, (n.d.). [http://whqlibdoc.who.int/publications/2011/9789241548151\\_eng.pdf](http://whqlibdoc.who.int/publications/2011/9789241548151_eng.pdf).
- [2] C.N.S. Commission, Tritium in drinking water, (n.d.). <http://nuclearsafety.gc.ca/eng/resources/health/tritium/tritium-in-drinking-water.cfm>.



- [3] PubChem, Tritiated Water, (n.d.). [https://pubchem.ncbi.nlm.nih.gov/compound/Tritiated\\_water#section=Top](https://pubchem.ncbi.nlm.nih.gov/compound/Tritiated_water#section=Top)
- [4] P. Elmer, MSDS for Ultima Gold, (n.d.). [http://www.perkinelmer.com/CMSResources/Images/44-149104lsc\\_process.JPG](http://www.perkinelmer.com/CMSResources/Images/44-149104lsc_process.JPG).
- [5] Y.H. T. Kawano H. Ohashi, E. Jamsranjav, Comparative Testing of Various Flow-Cell Detectors Fabricated Using CaF<sub>2</sub> Solid Scintillator, *Fusion Sci. Technol.* 67 (2015) 404–407.
- [6] T. Kawano, H. Ohashi, Y. Hamada, E. Jamsranjav, Shielding Effect On Tritium Water Monitoring System Based On CaF<sub>2</sub> Flow-Cell Detector, *Nucl. Sci. Tech.* 25 (2014) S010401-3.
- [7] T. Kawano, T. Uda, T. Yamamoto, H. Ohashi, Tritium Water Monitoring System Based on CaF<sub>2</sub> Flow-Cell Detector, *Fusion Sci. Technol.* 60 (2011) 952–955.
- [8] K. Shirahashi, G. Izawa, Y. Murano, Y. Muramastu, K. Yoshihara, Radio-Liquid Chromatography for Tritium Labelled Organic Compounds Using CaF<sub>2</sub>/Eu/ Scintillator, *J. Radioanal. Nucl. Chem.* 86 (1984) 1–9.
- [9] A.A.K. et al., CaF<sub>2</sub>-Eu Single-Crystal Scintillation Blocks for Detecting  $\beta$ -Radiation, *At. Energy.* 76 (1994) 191–194.
- [10] Shul-gin, Scintillation Detectors Working with CaF<sub>2</sub>-Eu Single Crystals, *At. Energy.* 75 (1993) 534–538.
- [11] M.J. Rudin, W.M. Richardson, P.G. Dumont, W.H. Johnson, In-situ Measurement of Transuranics using a Calcium Fluoride Scintillation Detection System, *J. Radiochem. Nucl. Chem.* 248 (2001) 445–448.
- [12] S. Gobain, NaI(Tl) and Polyscin<sup>®</sup> NaI(Tl) Sodium Iodide, (n.d.).
- [13] R.D. Evans, R.O. Evans, Studies of Self-Absorption in Gamma-Ray Sources, *Rev. Mod. Phys.* 20 (1948) 305–326. doi:10.1103/RevModPhys.20.305.
- [14] M.S. Badawi, M.M. Gouda, S.S. Nafee, A.M. El-Khatib, E.A. El-Mallah, New algorithm for studying the effect of self attenuation factor on the efficiency of gamma-rays detectors, *Nucl. Instruments Methods Phys. Res. Sect. A Accel. Spectrometers, Detect. Assoc. Equip.* 696 (2012) 164–170. doi:http://dx.doi.org/10.1016/j.nima.2012.08.089.
- [15] S.A. et al, Geant4-A Simulation Toolkit, *Nucl. Instruments Methods Phys. Res. Sect. A Accel. Spectrometers, Detect. Assoc. Equip.* 506 (2003) 250–303.
- [16] N.P. Laboratory, Kaye and Laby, (n.d.). <http://www.kayelaby.npl.co.uk/>.
- [17] R. Burek, D. Chocyk, Basic Aspects Of The Mass Absorption Coefficient Of Beta Particles, *J. Radioanal. Nucl. Chem.* 209 (1996) 181–191.
- [18] G.P. Lepage, A New Algorithm For Adaptive Multidimensional Integration, *J. Comput. Phys.* 27 (1978) 192–203.
- [19] Python, Vegas 3.0 : Python Package Index, (n.d.). <https://pypi.python.org/pypi/vegas>.
- [20] N.J.D. Nagelkerke, A Note On A General Definition Of The Coefficient Of Determination, *Biometrika.* 78 (1991) 691–692.
- [21] CERN, Electromagnetic Standard Physics Working Group, (n.d.). [https://geant4.web.cern.ch/geant4/collaboration/working\\_groups/electromagnetic/](https://geant4.web.cern.ch/geant4/collaboration/working_groups/electromagnetic/).
- [22] C. for Radiation Protection Knowledge, Rad Toolbox v. 3.0.0, (n.d.). <https://crpk.ornl.gov/software/>.
- [23] N. Yoder, Matlab Peakfinder, (n.d.). <https://www.mathworks.com/matlabcentral/fileexchange/25500-peakfinder-x0--sel--thresh--extrema--includeendpoints--interpolate->.
- [24] F. Corsi, A. Dragone, C. Marzocca, A. Del Guerra, P. Delizia, N. Dinu, C. Piemonte, M. Boscardin, G.F.D. Betta, Modelling a silicon photomultiplier (SiPM) as a signal source for optimum front-end design, *Nucl. Instruments Methods Phys. Res. Sect. A Accel. Spectrometers, Detect. Assoc. Equip.* 572 (2007) 416–418. doi:http://dx.doi.org/10.1016/j.nima.2006.10.219.
- [25] F. Corsi, M. Foresta, C. Marzocca, G. Matarrese, A. Del Guerra, ASIC development for SiPM readout, *J. Instrum.* 4 (2009) P03004. <http://stacks.iop.org/1748-0221/4/i=03/a=P03004>.